Thermodynamic Analysis of a Poly-generation System for Electrical Power, Cooling and Desalinated Water

Ayman O. ABDELHAY[1,2], Hassan E. S. FATH[3], Sameh A. NADA[4], Mohamed A. SHARAF[5]

[1]Faculty of Engineering, Egypt-Japan University of Science and Technology, New Borg El-Arab City, Alexandria, Egypt, ayman.osama@ejust.edu.eg
[2] Faculty of Engineering, Menoufia University, Shebin El-Kom, Menoufia, Egypt, ayman.osama@sh-eng.menofia.edu.eg
[3] Faculty of Engineering, Egypt-Japan University of Science and Technology, New Borg El-Arab City, Alexandria, Egypt, hassan.fath@ejust.edu.eg
[4] Faculty of Engineering, Egypt-Japan University of Science and Technology, New Borg El-Arab City, Alexandria, Egypt, sameh.nada@ejust.edu.eg
[5] Department of Engineering Science, Faculty of Petroleum & Mining Engineering, Suez University, Egypt, mohammed.eldeen@suezuniv.edu.eg, mwahab31@yahoo.com

Abstract:

Nowadays, designing new poly-generation systems is needed to meet the increasing communities demands of electrical energy, space cooling and fresh water. This should take more attention especially with the increasing conventional fossil fuel energy costs, freshwater shortage and CO2 emission. This work presents the thermodynamic analysis of a sustainable poly-generation thermal system that can produce electricity, space cooling and desalinated water. The proposed system combines a Concentrated Solar Power (CSP), Steam Rankine Cycle (SRC), Multi Effect Distillation (MED) system and Absorption Refrigeration System (ARS). The system design target is to provide communities in remote areas with all needs of water, electricity and cooling using low-grade heat from green solar energy. In the solar field, solar irradiation is collected by Parabolic Trough Collectors (PTC) to heat the working fluid (Therminol-VP1 heat transfer oil). Thermal oil transfers the absorbed heat to the SRC that generates the required electrical power and provides both MED and ARS with a proper heating steam required depending on the demand loads. The developed model is used to design a pilot test unit of 10 kW electrical power, 1.7 m^3/day of desalinated water and 3.6 TR cooling load capacity. flow, heat, and exergy destruction rates for each component of the system are obtained. Performance parameters of the subsystems forming the plant are also evaluated. Results revealed that the PTC represent the most critical part in the system from the exergetic point of view as it experiences 84.65% of the total system exergy destruction the required PTC area is 83.12 m^2. For the ARS unit, exergy loss is about 2.2 kW, 36.22% and 28.87% of this value occur in absorber and generator respectively. MED unit simulation results demonstrated that the gain ratio and specific heat transfer area are 2.29 and 144 m^2/kg/s respectively. The exergy destruction in the MED unit is 1.8244 kW (66.43% in evaporators and 33.57%in condenser). The ARS coefficient of performance and second law efficiency were 0.7755 and 59.24% respectively.

Keywords: Polygeneration, MED, CSP, Absorption

1. INTRODUCTION

Earth has a tremendous amount of water nevertheless, only 2.5% is pure water and the rest is salty. Therefore, to produce drinkable water from the dramatically available salty water, different desalination methods have been invented and used depending on the process energy, efficiency and cost. In the last decades, seawater desalination installed capacity has grown sharply and increased from 22 Mm^3/day in 2000 up to more than 90 Mm^3/day in 2015 (Saldivia *et al.*, 2019). A considerable part of this production capacity is covered by thermal desalination techniques especially for relatively large water production capacities (Ettouney and El-Dessouky, 1999). Thermal desalination has high energy consumption compared to membrane processes in which 130 million tons of oil fuel can be used for annual water production of 13 Mm^3/day (Kalogirou, 1997; Kouhikamali and Mehdizadeh, 2011) which will cause a huge production of CO_2 emissions. At the same time, utilization of solar energy, instead of fossil fuels, to provide such desalination systems with the required energy can play a key role in decreasing the bad environmental impact of CO_2 emissions and the rejected waste heat.

Applying the cogeneration systems to produce both fresh water and electricity driven by solar energy can solve both energy and water shortages, and decline the unit water and power cost as well (Palenzuela, Zaragoza and Alarcón-Padilla, 2015). Therefore, to cover the growing demand of potable water and electricity in an economical way, solar cogeneration systems for power and desalination can be utilized (Fernández-Izquierdo *et al.*, 2012). Multi-Effect Desalination (MED) method is considered one of the most convenient techniques to be coupled with solar systems due to it's potential to be supplied by low-grade heat sources (lower than 70°C) in addition, it has lower capital cost and pumping power compared to the other thermal desalination systems (Wang and Lior, 2006). Many articles have performed energy, exergy and economic analyses beside the optimization of MED process in order to investigate and optimize different parameters that affect system design and performance (Ji *et al.*, 2007; Kamali and Mohebinia, 2008; Nafey, Fath and Mabrouk, 2008; Trostmann, 2009; Sayyaadi and Saffari, 2010; Shakib, Amidpour and Aghanajafi, 2011).

Regarding the solar MED systems (Thermal and Mechanical Vapor Compression, TVC, MVC), exergy and thermo-economical analyses have been investigated by (Sharaf, Nafey and García-Rodríguez, 2011a, 2011b). Comparisons between one purpose (water only) solar MED and dual-purpose (water and power) solar Organic Rankine Cycle (ORC)-MED systems were held. Moreover, comparison between Therminol-VP1 and Toluene oils as a heat transfer fluid for the solar filed were also implemented. Results showed that the one purpose system is more economic than dual-purpose due to the higher gain ratio and lower Parabolic Trough Collector (PTC) area needed. Also, results revealed that increasing the number of MED evaporators reduces each of the solar field area, specific power consumption and unit product cost. System gain ratio can be increased by coupling of the TVC to the MED system instead of increasing the number of MED effects.

Also, (Saldivia *et al.*, 2019) presented a thermodynamic simulation model for a combined MED-solar steam generation plant (PTC collectors, a storage tank, and a steam generator) system under different operating conditions. The developed model showed a good agreement with the compared data obtained from Plataforma Solar de Almería (PSA) in Spain. Results showed that system water productivity increases linearly with solar radiation intensity. It was also concluded that the investigated model can be a powerful tool for the design and optimization of solar MED systems.

MED system can be also driven by Linear Fresnel (LF) concentrating solar power instead of using PTCs. Concerning this, (Hamed *et al.*, 2016) investigated the effect of thermal energy storage, direct normal irradiance, and fuel cost on the performance of MED system supplied by LF solar field. Results displayed that the LF-MED without thermal energy storage can be more economical under certain weather conditions. On the other hand, three different configurations of LF-MED/TVC were studied techno-economically by (Askari and Ameri, 2016). System and water production costs were assessed in addition to the annual fuel savings and size of LF solar field. Results showed that the water production cost was 1.63 $/$m^3$ but, it increases to 3.09 $/$m^3$ in case of providing system with thermal storage. If the thermal storage duration increases from 6 h to 12 h, water production costs rises by about 42% and 65%, respectively.

In the last two decades, and, due to the dramatic growth in residential and commercial buildings, cooling loads have become a major consumer of electricity during summer due to the use of traditional vapor compression air conditioning devices (Lee and Sherif, 2001). As the energy shortage increases year by year, application of heat-driven refrigeration systems could be considered as appropriate alternative. Absorption systems are characterized by the possibility of utilizing low-grade heat, which is rejected normally to the environment from the power cycles, to produce chilled water and/or hot water for both cooling and heating applications. In hot dry regions, it is reasonable to use systems that produce both chilled and pure water. Some articles studied the integration of air conditioning and HDH systems for building cooling and fresh water production (Nada, Elattar and Fouda, 2015b, 2015a; Elattar, Fouda and Nada, 2016; Fouda, Nada and Elattar, 2016). In addition, some researches proposed the combination of Absorption Refrigeration System (ARS) and MED systems in which both systems can work by low temperature heat source. (Aly, 1995) introduced a novel hybrid system combining LiBr-H_2O absorption system and 20 effects vertical stack MED distillation system for a capacity of 1.53 MGD of drinkable water with a GOR of

14.8 in addition to 3000 TR cooling. The performed analysis revealed that the proposed plant offers low cost water because the MED top brine temperature can be lowered to (30°C).

While, the hybrid single/double stage ammonia-water ARS combined with MED were investigated by (Alelyani *et al.*, 2017). The absorption system rectifier heat rejection which is supplied to the MED system. Thermodynamic and economic analyses were performed using Engineering Equation Solver (EES) software. The influence of concentration difference of strong and weak solutions, temperature of absorber and evaporator, and number of MED evaporators on the system gained ratio, cooling and water capacity, and exergy efficiency were studied. Results demonstrated that the exergy degradation of the proposed hybrid system is lower than stand-alone ARS or MED systems by about 55%. Coupling single and double stage ARS to the MED causes water production cost to decline by 30% and 9% respectively. Comparison between single and double stage ARS-MED and stand-alone ARS revealed that the cooling capacity decreases by 16% for the single-stage and remains constant for the two-stage system. The water unit product cost (UPC, $/m3) has increases by 19% single-stage system and by 3% for the double-stage one while, the cooling UPC reduced by 44% due to the ARS-MED coupling.

Recently, several novel hybrid systems have been performed in order to face the problem of the increasing demands of energy, cooling, heating and freshwater issues. These systems are called poly-generation systems. Poly-generation systems aim also to decrease the environmental pollution related to the use of fossil fuels and the rates of CO_2 emissions through the partial or total replacement of fossil fuels by renewable energy sources. Furthermore, these integrated systems help in reducing the overall heat losses and increasing the amount of economic saving.

Some research works were found to deal with the poly-generation systems. (Calise, Dentice d'Accadia and Piacentino, 2014) introduced a poly-generation system combining photovoltaic/thermal (PVT) solar collectors, biomass fuelled heater, MED and ARS (single-stage LiBr-H_2O) to generate electricity, potable water, heating and cooling. PVT produces both electricity to the main grid and heat supply for the ARS unit. The MED unit was provided by heat from the solar field and the biomass heater. Dynamic simulation was carried out using TRNSYS program. The conducted thermoeconomic analysis indicated that the optimum solar field area for the ARS system is about 5.9 m^2/kW. The storage tank volume was suggested to be 15 Litre/m^2 of solar field. Forthermore, the optimum number of effects of MED unit was 14. The most convenient temperatures at the solar field outlet temperatures in summer and winter was 85°C and 55°C respectively.

(Calise *et al.*, 2014) presented a hybrid MED-ARS (single-stage LiBr–H2O) powered by geothermal energy and concentrating photovoltaic/thermal solar collectors to produce electricity, thermal energy, cooling energy and fresh water simultaneously. The absorption chiller is powered by the thermal energy produced by the solar field (100°C). While, the MED system is driven by heat from the geothermal fluid (80°C). TRNSYS package was utilized to perform a dynamic simulation of the proposed system. Results showed that the energetic performance of the proposed system during summer is much better than during winter. The implemented economic analysis showed that the system profitability rises considerably with the hot water load increase. Simple payback period periods may increase to 10 years in case of lower utilization of thermal energy, but full utilization of energy and water causes the pay back periods to decrease significantly.

(Calise *et al.*, 2017) proposed the poly-generation combining MED, ORC and ARS supplied by energy from PTC solar field and geothermal wells. The studied system produces electricity, potable water in addition to cooling and heating energies. TRNSYS environment was used to implement one-year dynamic simulation using data of Pantelleria Island. Appropriate temperature for each component to avoid the very small temperature of the reinjected fluid to the geothermal wells was investigated. Electrical load was attained from measured data while heating and cooling loads were calculated by building dynamic simulation. Results showed that the studied system can supply 800 buildings with energy and water needs. The plant annual production was assessed to be 5120 MWh electricity, 1006 Mm^3 of pure water. Efficiency of the ORC was 15.30%, if the ORC uses (14.6%) solar energy and (85.4%) geothermal energy. The economic and environmental results indicated that the simple payback period was 8.5 while, the avoided fossil fuel and CO_2 emissions were estimated to be 3039 and 9451 tons respectively.

(Sahoo *et al.*, 2015) proposed a poly-generation system in which both biomass and solar energy were utilized to produce steam required for the electric power production (through steam turbine) and to supply an ARS with the required heat. Then, through a heat exchanger, the waste heat rejected from the ARS condenser is transmitted a multi effect humidification-dehumidification desalination system. Thermodynamics analysis of the proposed plant introduced poly-generation system that been carried out based on the Indian climatic condition (ambient temperature was assigned as 35°C). Analysis demonstrated that the proposed integration enhances the overall system efficiency and significantly decrease CO_2 emissions as well.

As there are too many systems that can separately produce power, cooling, heating and desalinated water, there will be a lot of integrations that can be suggested for study and investigation. This article represents an introduction of one of these new integrated systems. In this study, a poly-generation system driven by solar energy and producing simultaneously electricity, cooling energy and pure water will be presented. The suggested system is an integration of concentrated solar power system (using PTCs), steam Rankine cycle (SRC), multi effect desalination

(MED) system and absorption refrigeration system (ARS) as shown in Figure 1. System design will be investigated using energy and exergy concepts. Furthermore, the simulation results will be presented.

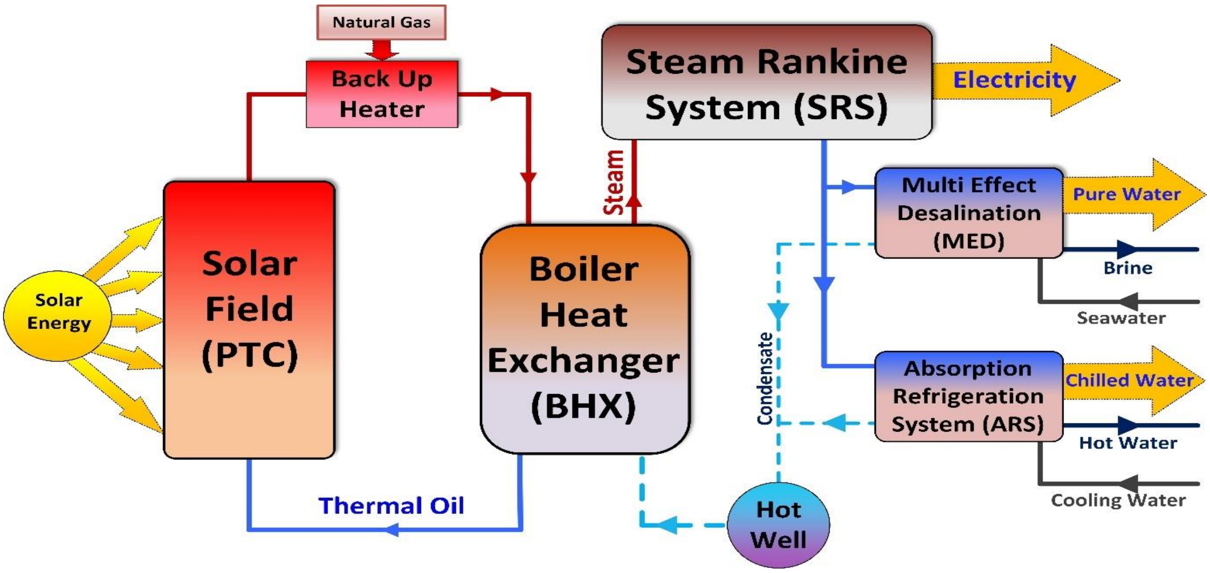

Figure 1: Flow diagram of the proposed Poly-generation System for Electricity, Cooling and Pure Water

2. AIM OF THE STUDY

In the present work, steady state energetic and exergetic design techniques of modeling are performed for a PTC-SRC-MED-ARS poly-generation system powered by solar energy. Up to authors knowledge, no article available in literature dealt with the proposed integration from that side. The poly-generation plant introduced in this work is suitable for medium and high loads of electricity, cooling and potable water production. This may be reasonable for coastal and tourist spots along the solar beam areas like Middle East, North Africa (MENA) and GULF regions.

The studied system components are modeled and simulated depending on both first and second laws of thermodynamics using MATLAB environment. As a first step in modeling this system, the study is implemented depending on steady state basis at a constant value of solar radiation intensity. This work aims to present and analyze the thermal design results gained for the proposed plant in order to produce 10 kWe power, 1.7 m^3/day of pure water and 3.6 TR cooling. These small capacities have been chosen to suit a small plant that can be afterwards assembled and installed to study the proposed system feasibility. The energetic and exergetic results will be presented and discussed.

3. SYSTEM LAYOUT

As mentioned previously, the proposed layout combines three sub-systems, solar power system, absorption refrigeration system (ARS) and multi-effect distillation (MED) unit. The solar power system includes concentrated solar power cycle and steam Rankine cycle. Basically, the plant is driven by solar energy but, during night or in case of solar irradiation reduction, an auxiliary natural gas fueled heater is utilized to stabilize the working fluid temperature. The proposed plant can generate electricity, space cooling and desalinated water continuously. The plant is mainly composed of the four units that can be described in detail through the following sections.

3.1. Solar field loop description & design data

Solar field loop combines a set of PTCs, Natural gas heater and boiler heat exchanger. Therminol-VP1 thermal oil is employed as a working fluid. It can stay as a liquid phase under 400ºC (Sharaf Eldean and Soliman, 2015). Solar radiation is collected and concentrated on the thermal oil by parabolic trough collectors. Due to the continuous change in the solar radiation intensity, another energy source (gas fired heater) is used to compensate the decrease in the radiation intensity. Consequently, steady state condition for the boiler heat exchanger can be achieved. Through the boiler, heat gain is transferred from the thermal oil to the water side flowing in the Rankine cycle. In simulation solar intensity is assumed to be constant to accomplish the steady state condition. In order to design the solar field components (i.e. PTCs area, gas-fired heater and boiler capacity), input data shown in

Table 1,**Error! Reference source not found.** was specified in the developed MATLAB program.

3.2. Steam Rankine loop description & design data

Steam Rankine loop generates the necessary electrical power for the consumers. In the boiler heat exchange, superheated steam is formed due to the heat transfer with thermal oil. Then, steam is expanded in the turbine producing mechanical power that is converted into electrical power in generator. At the turbine outlet, steam is assumed to be wet with 85% quality in order to decrease steam temperature at the turbine inlet and to increase the turbine life span. The back-pressure steam rejected from the turbine is exploited to drive both MED and ARS units instead of losing its energy through the condenser. The condensate rejected from the MED and ARS is collected in the condenser hot well and pumped again to the boiler. In case of MED and ARS part load, the remaining steam is condensed in the condenser. The design input data for the steam Rankine cycle are illustrated in

Table 1.

Table 1 Design Data for Solar Field loop and Steam Rankine Cycle

Solar Field Loop			Steam Rankine Cycle		
Description	Value	Unit	Description	Value	Unit
Solar irradiation	750	W/m^2	Electrical power output	10	kW
Boiler effectiveness	80%	-	Turbine efficiency	85%	-
Natural gas heater efficiency	70%	-	Turbine outlet steam dryness fraction	85%	-
Natural gas calorific value	42000	kJ/kg	Electrical generator efficiency	90%	-
Therminol-VP1 maximum temperature	350	˚C	Pump efficiency	85%	-
			Condenser temperature difference	10	˚C

3.3. MED unit description & design data

In the MED unit, turbine steam condenses completely inside the tubes of the first effect (evaporator). While the feed saline water (sprayed outside the tubes) boils and generate another amount of steam. Steam outlet of each effect serves as an energy source for the next effect. On the other hand, the rejected concentrated brine from each effect is directed to the next effect (at lower pressure) to generate more steam by flashing. Then at the end condenser, steam of the final effect condensed due to cooling by sea water. Part of the heated seawater is used as feed water to effects and the other part is returned back to the sea. The condensed pure water from each effect is collected as the required output desalinated water. The design data of MED system is summarized in Table 2.

3.4. ARS unit description & design data

The ARS unit is a single stage Water-LiBr type. This type is selected due to its better performance compared to ammonia-water solution (Horuz, 1998). Turbine steam condensation in the ARS generator results in boiling of Water-LiBr solution and separation of the refrigerant (water vapor). Then, weak solution is returned through a throttle valve to the absorber. In the ARS condenser, heat is removed from the refrigerant to the cooling water. Refrigerant is then throttled to fulfill the required temperature at the evaporator in which the chilled water acquires its low temperature needed for the cooling application. The evaporated refrigerant is cooled, condensed and mixed with the LiBr in the absorber forming a strong solution. Finally, the strong solution is pumped back to the generator and so on. To enhance the ARS performance, strong and weak solutions exchanges heat through liquid-liquid heat exchanger (Sözen, 2001). Input design data is displayed in Table 2.

Table 2 Design data for MED unit and ARS unit

MED unit			ARS unit		
Description	Value	Unit	Description	Value	Unit
Water production capacity	1700	kg/day	Cooling load	3.6	TR
Number of effects	3	-	Generator outlet temperature	88	˚C
Heating steam temperature	69	˚C	Absorber outlet temperature	30	˚C
Feed seawater salt concentration	35000	ppm	Refrigerant outlet temperature from condenser	38	˚C
Rejected brine salt concentration	65000	ppm	Evaporator temperature	4	˚C
Feed seawater temperature	25	˚C	Chilled water inlet temperature	12	˚C
Effects feed water temperature	10	˚C	Chilled water outlet temperature	6.5	˚C
			Cooling water inlet temperature (to absorber)	25	˚C
			Cooling water outlet temperature	35	˚C

	Heat exchanger effectiveness	65%	-

4. SIMULATION RESULTS AND DISCUSSION

A user–friendly graphical interface (GUI) for the proposed system has been developed using MATLAB toolbox environment. Through it, the required output capacities (electricity, cooling and water) and design initial values can be given as input data then, the simulation results can be calculated and displayed directly as shown in Figure 2. The presented simulation results are based on 10 kW electrical power, 1.7 m^3/day and 3.6 TR cooling capacity. Results include streams flow rate, temperatures, performance parameters and exergy destruction of different system parts. The detailed simulation results are introduced in the following sections.

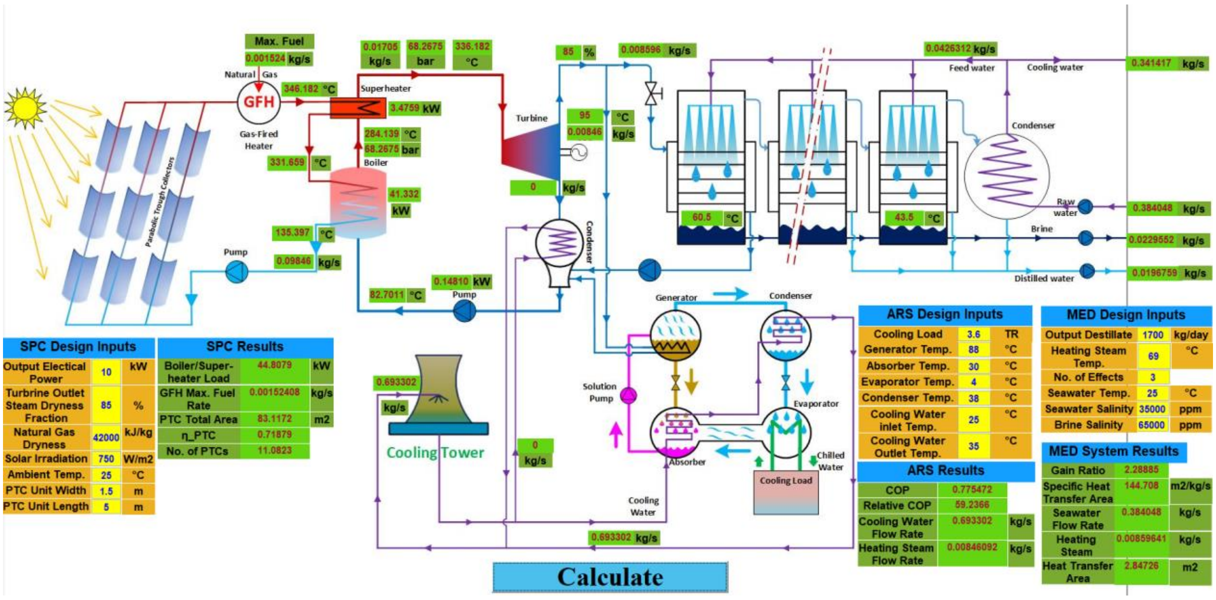

Figure 2: Developed GUI Simulation Results

4.1. Solar power system simulation results

Solar Power System (SPS) combines the solar field and steam Rankine loops. Simulation results for the SPS are introduced in Table 3. Streams flow rate and components capacities are calculated. PTC thermal efficiency as well as the required PTC area are computed to be 71.88% and 83.12 m^2. Exergy destruction analysis showed that the most critical part in the system that causes the highest percent of the exergy destruction is the PTCs. It represents 67.77% of the solar exergy input and 92.67% of the SPS exergy destruction as Table 3 demonstrates. In addition, as can be seen in Figure 3, PTC exergy loss accounts for 84.72% of the total system exergy destruction.

Table 3 Energetic and Exergetic Results of Solar Power System

Description	Value	Unit	Description	Value	Unit
Turbine steam flow rate	0.0171	kg/s	Solar energy exergy input	58.0676	kW
Condenser maximum heat rate	32.9063	kW	Exergy destruction in turbine	1.5871	kW
Condenser maximum cooling water flow rate	0.7872	kg/s	Exergy destruction in boiler heat exchanger	1.4867	kW
Boiler heat exchanger capacity	44.8079	kW	Exergy destruction in hot well	0.0138	kW
Thermal oil flow rate	0.0985	kg/s	Exergy destruction in pump	0.0246	kW
Gas fired heater fuel capacity	0.0015	kg/s	Exergy destruction in PTC	39.3538	kW
PTC thermal efficiency	71.88%	-	Exergy destruction in solar power system	42.4660	kW
PTC area	83.1172	m^2			

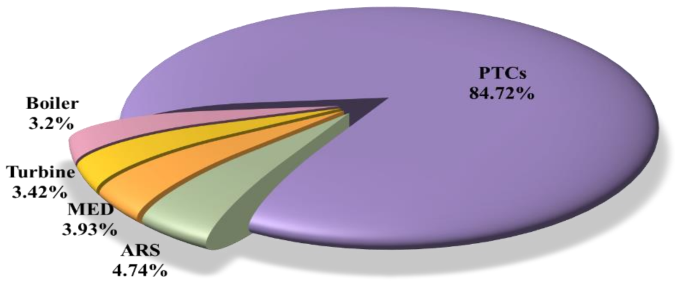

Figure 3: Plant Exergy Destruction analysis results by percentage

4.2. MED simulation results

Simulation results for the MED unit generating 1.7 m^3/day are presented in Table 4. Flow rates of inlet and outlet streams of the system are determined. Heat transfer area and exergy destruction of effects and condenser are evaluated. Then the system gain ratio (GR) (kg desalinated water/ kg heating steam) and specific heat transfer area (m2/kg/s desalinated water) are computed as 2.29 and 144 respectively. Total exergy destruction in the MED system is evaluated to be 1.8244 kW or 3.93% of the total plant exergy destruction (Figure 3). Exergy analysis, shown in Figure 4, also showed that each effect and condenser account for 22.14% and 33.57% of the MED total exergy destruction respectively.

Table 4 Energetic and Exergetic Results of MED Unit

Description	Value	Unit	Description	Value	Unit
Heating steam flow rate	0.0086	kg/s	Total heat transfer area for MED	2.8473	m^2
Seawater flow rate	0.3840	kg/s	Exergy destruction per effect	0.404	kW
Feed flow rate to effects	0.0426	kg/s	Exergy destruction in condenser	0.6125	kW
Rejected brine flow rate	0.0230	kg/s	Total exergy destruction in MED	1.8244	kW
Heat transfer area per effect	0.8115	m^2	Gain ratio	2.2889	-
Condenser heat transfer area	0.4129	m^2	Specific heat transfer area	144.7077	m^2/(kg/s)

4.3. ARS simulation results

Table 5 illustrates thermodynamic simulation results of the ARS unit. Heat rates of ARS parts including generator, condenser, Absorber and heat exchanger are presented. Unfortunately, no available correlations were found in the literature to calculate the heat transfer area of these parts directly. Table 5 displays also mass flow rates of the heating steam, strong and weak solutions, cooling water and Chilled water. Exergy destruction for each part of the ARS were calculated. For the entire ARS, exergy destruction accounts for 2.2015 kW or 4.74% of the plant Exergy loss (Figure 3). While, the highest exergy loss experiences in the absorber and generator by 36.22% and 28.87% respectively (Figure 4). Therefore, a special attention must be considered in the design of these components. On the other hand, the exergy destruction in evaporator and condenser are 15.39% and 13.2% respectively. System coefficient of performance and second law efficiency were calculated to be 0.7755 and 59.24% respectively as mentioned Table 5.

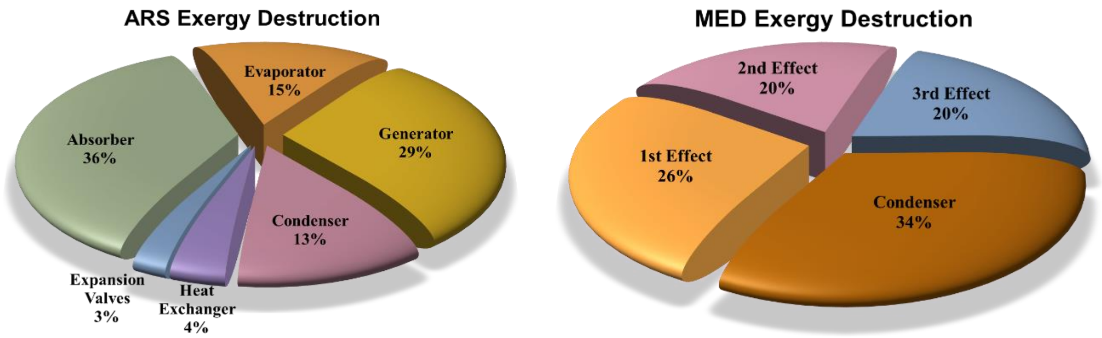

Figure 4: ARS and MED Exergy Destruction analysis results by percentage

Table 5 Energetic and Exergetic Results of ARS Unit

Description	Value	Unit	Description	Value	Unit
Generator Heat Rate	16.3224	kW	Exergy Destruction in Absorber	0.7973	kW
Condenser Heat Rate	13.348	kW	Exergy Destruction in Evaporator	0.3388	kW
Absorber Heat Rate	15.632	kW	Exergy Destruction in Generator	0.6355	kW
Heat Exchanger Rate of Heat	2.0927	kW	Exergy Destruction in Condenser	0.2906	kW
Steam Flow Rate of ARS	0.0085	kg/s	Exergy Destruction in Heat Exchanger	0.0852	kW
Chilled Water flow rate	0.545	kg/s	Exergy Destruction in Expansion Valves	0.0541	kW
Cooling Water Flow Rate	0.6933	kg/s	Total Exergy Destruction in ARS Unit	2.2015	kW
Refrigerant flow rate	0.0054	kg/s	Coefficient of Performance	0.7755	-
Strong Solution flow rate	0.0353	kg/s	Maximum Coefficient of Performance	1.3091	-
Weak Solution flow rate	0.0299	kg/s	Second Law Efficiency	59.24%	-

4.4. Exergy analysis summary

Figure 5 presents the exergy balance diagram including the values of exergy input mainly with the solar energy, the exergy destruction of the whole plant and different system components, and the exergy output with the turbine mechanical power and with the outlet streams. The highest exergy destruction occurred in the PTC is due to the big difference between the highest exergy input, as it depends on the sun temperature (5800k), and the exergy output due to the heat transfer to the thermal oil. Consequently, in order to decrease the PTC exergy loss, the heat transfer between the solar radiation and the thermal oil has to be enhanced through new designs and investigations.

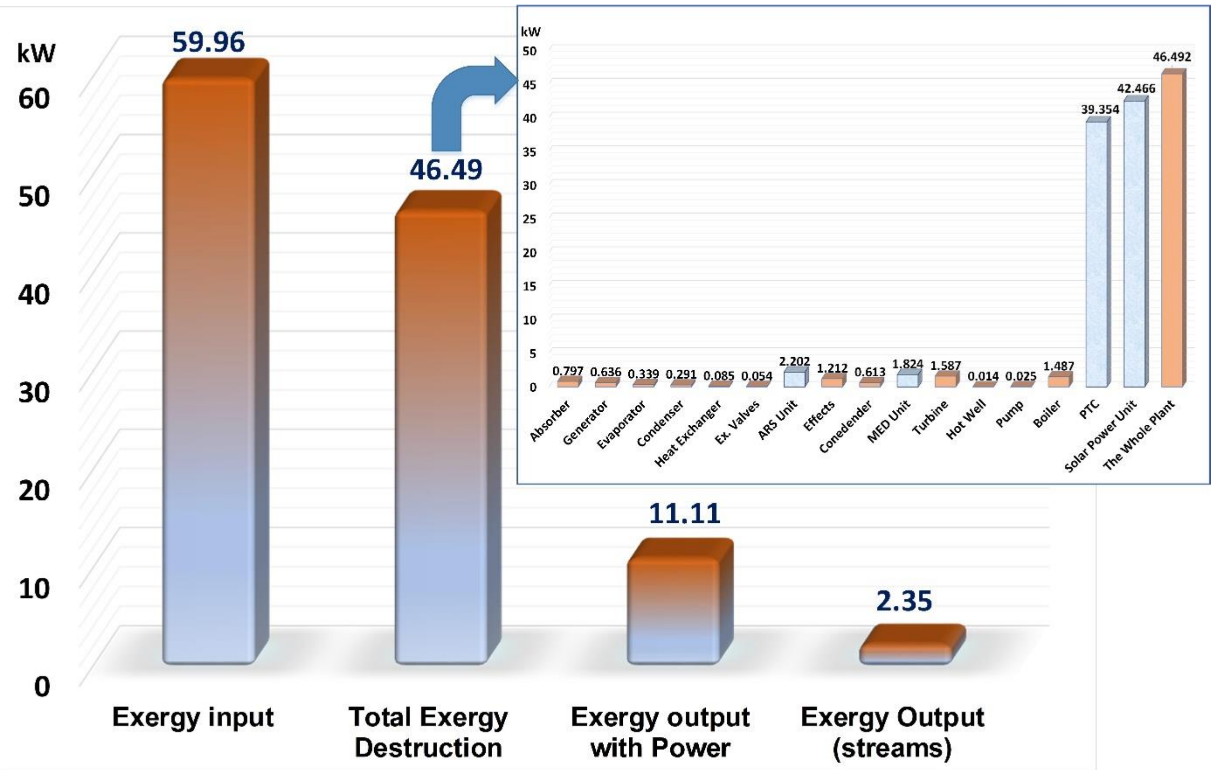

Figure 5: Exergy balance diagram

5. CONCLUSIONS

This study introduced a novel poly-generation capable to produce electrical power, cooling and desalinated water. The proposed plant is powered by concentrated solar power. System configuration combine PTC solar field, steam Rankine cycle, MED system and absorption chiller. System modelling depending on both first and second laws of thermodynamics is performed using MATLAB package. A case study of 10 kWe power, 1.7 m^3/day of desalinated water and 3.6 TR cooling is applied to the simulation program. Energetic and exegetic results have been presented and revealed that:

- The required PTC area for the studied plant is 83.12 m^2 with a thermal efficiency of 71.88%.
- PTC experiences the highest exergy destruction (39.3538 kW) compared to other system components. It represents about 84.65% of the total system exergy destruction and 67.77% of the solar exergy input.
- The MED gain ratio GR and specific heat transfer area are evaluated to be 2.29 and 144 respectively.
- MED system records an exergy loss of 1.8244 kW (22.14% in each effect and 33.57% in condenser).
- Absorption chiller coefficient of performance and second law efficiency are 0.7755 and 59.24%.
- The total rate of exergy destruction of the ARS is 2.2 kW. Most of this value occurs in absorber and generator (36.22% and 28.87% respectively).
- To overcome the high exergy destruction in the PTC, heat transfer to the thermal oil has to be modified through new designs and investigations.

6. REFERENCES

Alelyani, S. M. *et al.* (2017) 'Techno-economic analysis of combined ammonia-water absorption refrigeration and desalination', *Energy Conversion and Management*. Elsevier Ltd, 143, pp. 493–504. doi: 10.1016/j.enconman.2017.03.085.

Aly, S. E. (1995) 'A study of a new thermal vapor compression/multi-effect stack (TVC/MES) low temperature distillation system', *Desalination*, 103(3), pp. 257–263. doi: 10.1016/0011-9164(95)00078-X.

Askari, I. B. and Ameri, M. (2016) 'Techno economic feasibility analysis of Linear Fresnel solar field as thermal source of the MED/TVC desalination system', *Desalination*. Elsevier B.V., 394, pp. 1–17. doi: 10.1016/j.desal.2016.04.022.

Calise, F. *et al.* (2014) 'A novel renewable polygeneration system for a small Mediterranean volcanic island for the combined production of energy and water: Dynamic simulation and economic assessment', *Applied Energy*. Elsevier Ltd, 135, pp. 675–693. doi: 10.1016/j.apenergy.2014.03.064.

Calise, F. *et al.* (2017) 'A novel hybrid polygeneration system supplying energy and desalinated water by renewable sources in Pantelleria Island', *Energy*. Elsevier Ltd, 137, pp. 1086–1106. doi: 10.1016/j.energy.2017.03.165.

Calise, F., Dentice d'Accadia, M. and Piacentino, A. (2014) 'A novel solar trigeneration system integrating PVT (photovoltaic/thermal collectors) and SW (seawater) desalination: Dynamic simulation and economic assessment', *Energy*. Elsevier Ltd, 67, pp. 129–148. doi: 10.1016/j.energy.2013.12.060.

Elattar, H. F., Fouda, A. and Nada, S. A. (2016) 'Performance investigation of a novel solar hybrid air conditioning and humidification-dehumidification water desalination system', *Desalination*. Elsevier B.V., 382, pp. 28–42. doi: 10.1016/j.desal.2015.12.023.

Ettouney, H. M. and El-Dessouky, H. (1999) 'A simulator for thermal desalination processes', *Desalination*, 125(1–3), pp. 277–291. doi: 10.1016/S0011-9164(99)00148-4.

Fernández-Izquierdo, P. *et al.* (2012) 'Experimental analysis of a multi-effect distillation unit operated out of nominal conditions', *Desalination*. Elsevier B.V., 284, pp. 233–237. doi: 10.1016/j.desal.2011.09.004.

Fouda, A., Nada, S. A. and Elattar, H. F. (2016) 'An integrated A/C and HDH water desalination system assisted by solar energy: Transient analysis and economical study', *Applied Thermal Engineering*. Elsevier Ltd, 108, pp. 1320–1335. doi: 10.1016/j.applthermaleng.2016.08.026.

Hamed, O. A. *et al.* (2016) 'Concentrating solar power for seawater thermal desalination', *Desalination*. Elsevier B.V., 396, pp. 70–78. doi: 10.1016/j.desal.2016.06.008.

Horuz, I. (1998) 'a comparison between ammonia - water and water - lithium bromide solutions in vapor absorption refrigeration systems', *International Communications in Heat and Mass Transfer*, 25(5), pp. 711–721.

Ji, J. G. *et al.* (2007) 'Simulation and analysis of a single-effect thermal vapor-compression desalination system at variable operation conditions', *Chemical Engineering and Technology*, 30(12), pp. 1633–1641. doi: 10.1002/ceat.200700303.

Kalogirou, S. (1997) 'Survey of solar desalination systems and system selection', *Energy*, 22(1), pp. 69–81. doi: 10.1016/S0360-5442(96)00100-4.

Kamali, R. K. and Mohebinia, S. (2008) 'Experience of design and optimization of multi-effects desalination systems in Iran', *Desalination*, 222(1–3), pp. 639–645. doi: 10.1016/j.desal.2007.01.182.

Kouhikamali, R. and Mehdizadeh, M. S. M. (2011) 'Process investigation of different locations of thermo-compressor suction in MED-TVC plants', *Desalination*. Elsevier B.V., 280(1–3), pp. 134–138. doi: 10.1016/j.desal.2011.06.070.

Lee, S. F. and Sherif, S. A. (2001) 'Thermodynamic analysis of a lithium bromide/water absorption system for cooling and heating applications', *International Journal of Energy Research*, 25(11), pp. 1019–1031. doi: 10.1002/er.738.

Nada, S. A., Elattar, H. F. and Fouda, A. (2015a) 'Experimental study for hybrid humidification-dehumidification water desalination and air conditioning system', *Desalination*, 363, pp. 112–125. doi: 10.1016/j.desal.2015.01.032.

Nada, S. A., Elattar, H. F. and Fouda, A. (2015b) 'Performance analysis of proposed hybrid air conditioning and humidification-dehumidification systems for energy saving and water production in hot and dry climatic regions', *Energy Conversion and Management*. Elsevier Ltd, 96, pp. 208–227. doi: 10.1016/j.enconman.2015.02.082.

Nafey, A. S., Fath, H. E. S. and Mabrouk, A. A. (2008) 'Thermoeconomic design of a multi-effect evaporation mechanical vapor compression (MEE-MVC) desalination process', *Desalination*, 230(1–3), pp. 1–15. doi: 10.1016/j.desal.2007.08.021.

Palenzuela, P., Zaragoza, G. and Alarcón-Padilla, D. C. (2015) 'Characterisation of the coupling of multi-effect distillation plants toconcentrating solar power plants', *Energy*, 82, pp. 986–995. doi: 10.1016/j.energy.2015.01.109.

Sahoo, U. *et al.* (2015) 'Scope and sustainability of hybrid solar-biomass power plant with cooling, desalination in polygeneration process in India', *Renewable and Sustainable Energy Reviews*. Elsevier, 51(May), pp. 304–316. doi: 10.1016/j.rser.2015.06.004.

Saldivia, D. *et al.* (2019) 'Computational analysis for a multi-effect distillation (MED) plant driven by solar energy in Chile', *Renewable Energy*. Elsevier Ltd, 132, pp. 206–220. doi: 10.1016/J.RENENE.2018.07.139.

Sayyaadi, H. and Saffari, A. (2010) 'Thermoeconomic optimization of multi effect distillation desalination systems', *Applied Energy*. Elsevier Ltd, 87(4), pp. 1122–1133. doi: 10.1016/j.apenergy.2009.05.023.

Shakib, S. E., Amidpour, M. and Aghanajafi, C. (2011) 'A new approach for process optimization of a METVC desalination system', *Desalination and Water Treatment*, (October), pp. 84–96. doi: 10.5004/dwt.2012.2509.

Sharaf Eldean, M. a and Soliman, a M. (2015) 'Study of Using Solar Thermal Power for the Margarine Melting Heat Process.', *Journal of solar energy engineering*, 137(2), pp. 0210041–2100413. doi: 10.1115/1.4028367.

Sharaf, M. A., Nafey, A. S. and García-Rodríguez, L. (2011a) 'Exergy and thermo-economic analyses of a combined solar organic cycle with multi effect distillation (MED) desalination process', *Desalination*. Elsevier B.V., 272(1–3), pp. 135–147. doi: 10.1016/j.desal.2011.01.006.

Sharaf, M. A., Nafey, A. S. and García-Rodríguez, L. (2011b) 'Thermo-economic analysis of solar thermal power cycles assisted MED-VC (multi effect distillation-vapor compression) desalination processes', *Energy*. Elsevier Ltd, 36(5), pp. 2753–2764. doi: 10.1016/j.energy.2011.02.015.

Sözen, A. (2001) 'Effect of heat exchangers on performance of absorption refrigeration systems', *Energy Conversion and Management*, 42(14), pp. 1699–1716. doi: 10.1016/S0196-8904(00)00151-5.

Trostmann, A. (2009) 'Improved approach to steady state simulation of multi-effect distillation plants', *Desalination and Water Treatment*, 7(1–3), pp. 93–110. doi: 10.5004/dwt.2009.701.

Wang, Y. and Lior, N. (2006) 'Performance analysis of combined humidified gas turbine power generation and multi-effect thermal vapor compression desalination systems - Part 1: The desalination unit and its combination with a steam-injected gas turbine power system', *Desalination*, 196(1–3), pp. 84–104. doi: 10.1016/j.desal.2006.01.010.